Efficacy and Antivascular Effects of EphA2 Reduction With an Agonistic Antibody in Ovarian Cancer

Charles N. Landen Jr., Chunhua Lu, Liz Y. Han, Karen T. Coffman, Elizabeth Bruckheimer, Jyotsnabaran Halder, Lingegowda S. Mangala, William M. Merritt, Yvonne G. Lin, Changhou Gao, Rosemarie Schmandt, Aparna A. Kamat, Yang Li, Premal Thaker, David M. Gershenson, Nila U. Parikh, Gary E. Gallick, Michael S. Kinch, Anil K. Sood

Background: **EphA2 is an oncoprotein and tyrosine kinase receptor that is overexpressed in ovarian and many other cancers. We investigated the effects of reduced EphA2 levels on tumor growth and the tumor microenvironment in an orthotopic ovarian cancer model.** ***Methods:*** **The effect of the EphA2-agonistic monoclonal antibody EA5, alone or in combination with paclitaxel, on the growth of ovarian cancer cells (SKOV3ip1, HeyA8, and HeyA8MDR [taxane–platinum resistant]) was determined in vitro and in vivo by immunoblotting, 3-(4,5-dimethylthiazol-2-yl)-2,5-diphenyl tetrazolium bromide assay, and immunohistochemical analysis. Expression of EphA2 and markers of angiogenesis (CD31, vascular endothelial growth factor [VEGF], and basic fibroblast growth factor), proliferation (proliferating cell nuclear antigen), and endothelial cell apoptosis (CD31–terminal deoxynucleotidyl transferase biotin–deoxyuridine triphosphate nick-end labeling colocalization) and phosphorylation of Src were analyzed by immunoblotting, immunohistochemistry, immunofluorescence, and in situ hybridization in tumors from treated mice. Statistical tests were two-sided.** ***Results:*** **EA5 antibody treatment led to a more than 90% reduction in EphA2 expression in HeyA8 tumors in vivo. In mice bearing orthotopic SKOV3ip1 or HeyA8 tumors, 4 weeks of EA5 treatment resulted in tumors that weighed 31% and 45% less, respectively, than those in control (IgG-treated) mice (95% confidence interval [CI] = −0.09% to 71% and 20% to 70%, $P = .27$ and .01, respectively). Combination therapy with EA5 and paclitaxel reduced tumor weight by 77% and 80% (95% CI = 63% to 91% and 68% to 91%), respectively, compared with paclitaxel alone and by 92% and 88% (95% CI = 87% to 97% and 80% to 94%), respectively, compared with IgG alone. Combination therapy also reduced the weight of HeyA8MDR tumors by 47% (95% CI = 24% to 72%) compared with paclitaxel. Mice bearing SKOV3ip1 or HeyA8 tumors that were treated with combination therapy survived longer than those treated with paclitaxel alone (median survival = 144 versus 69 days and 46 versus 37 days, respectively). EA5-treated tumors had reduced microvascular density, proliferation, and VEGF protein and mRNA levels, with increased endothelial cell apoptosis. EphA2 was associated with Src, which was rapidly dephosphorylated after EA5 treatment.** ***Conclusions:*** **EA5 in combination with paclitaxel decreased tumor growth in an orthotopic ovarian cancer mouse model through antiangiogenic mechanisms associated with reduced levels of VEGF and phosphorylated Src. Humanized antibody constructs against EphA2 are worthy of future study. [J Natl Cancer Inst 2006;98:1558–70]**

Ovarian cancer remains the most common cause of death from gynecologic malignancy *(1)*. Approximately 75% of patients present with stage III or IV disease *(2,3)*, and the 5-year survival of such patients remains low, at 11%–31% *(1,3)*. Although most patients with advanced-stage disease will die of the disease, more than 70% have a favorable initial response to surgery and chemotherapy and a substantial fraction will respond to second-line therapies.

Biologically targeted therapies, such as cetuximab, bevacizumab, trastuzumab, and imatinib, have led to favorable responses in cancer therapy *(4–7)* and are being used in clinical trials for ovarian cancer. Many of these new compounds target receptor protein tyrosine kinases, which provide potent signals that often favor cell growth and survival. Among this class of targets, several independent lines of investigation have converged on the idea that the EphA2 receptor tyrosine kinase might provide a strong candidate for targeted intervention against cancer *(8–10)*. EphA2 was first linked with neuronal migration during embryonic development *(11–14)*. Subsequently, many tumor cells have been shown to overexpress this protein, and high levels of EphA2 are sufficient to promote many different aspects of a malignant phenotype, including proliferation, survival, migration, invasion, and angiogenesis *(9,15–21)*.

EphA2 overexpression has been observed in many human cancers, including lung, breast, prostate, colorectal, melanoma, and esophageal malignancies *(15,20,22–29)*. EphA2 overexpression is common in ovarian cancer, relates to disease severity, and is predictive of poor outcome in patients with ovarian cancer *(30)*. In addition, EphA2 overexpression leads to its constitutive association with a number of signaling molecules including focal adhesion kinase *(31)*, which is also commonly overexpressed in ovarian carcinomas *(30)*. Consistent with these findings, recent studies have demonstrated that reducing EphA2 levels is effective

Affiliations of authors: Departments of Gynecologic Oncology (CNL, CL, LYH, JH, LSM, WMM, YGL, RS, AAK, YL, PT, DMG, AKS) and Cancer Biology (NUP, GEG, AKS), The University of Texas M. D. Anderson Cancer Center, Houston, TX; MedImmune, Inc, Gaithersburg, MD (KTC, EB, CG, MSK).

Correspondence to: Anil K. Sood, MD, Departments of Gynecologic Oncology and Cancer Biology, The University of Texas M. D. Anderson Cancer Center, 1155 Herman Pressler, Unit 1362, Houston, TX 77030 (e-mail: asood@mdanderson.org).

See "Notes" following "References."

DOI: 10.1093/jnci/djj414

in reducing tumor growth in experimental models of ovarian, breast, and pancreatic cancers *(32–34)*.

One intriguing method of EphA2 reduction is through the use of agonistic antibodies *(33)*. These antibodies function in the same manner as ephrin-A1, the primary ligand for EphA2, in binding to the extracellular domain of EphA2, triggering receptor internalization and subsequent proteolysis *(35)*. Although most previous studies have focused on the direct effects of EphA2 antibodies on tumor cell growth and survival, we considered the possibility that reduced EphA2 levels could also exert effects on the local tumor microenvironment. To evaluate this hypothesis in the context of a physiologically relevant model, we investigated the antitumor effects of EphA2-agonistic antibodies using orthotopic ovarian cancer models. We also examined the effects of those antibodies on markers of angiogenesis and potential mechanisms by which antiangiogenic effects were mediated.

Materials and Methods

Cell Lines and Culture

The ovarian cancer cell lines HeyA8 and SKOV3ip1 were a kind gift of Dr Isaiah J. Fidler *(36)* and were maintained in RPMI-1640 supplemented with 15% fetal bovine serum (FBS) and 0.1% gentamycin sulfate (Gemini Bioproducts, Calabasas, CA). The HeyA8MDR cell line, a taxane-resistant line that was generated by sequential exposure to increasing concentrations of paclitaxel (Bristol-Myers Squibb, New York, NY), was maintained in the above media with 300 μg/mL of paclitaxel. Endothelial cells isolated from the mesentery or ovary of the immortomouse *(37)*, a kind gift of Dr Robert Langley, were maintained in Dulbecco's modified Eagle Medium with 10% FBS. These SV40-transformed cells proliferate indefinitely at 33 °C, but at 37 °C SV40 expression is inactivated and cells proliferate for only a few more cycles. These cells were maintained at 37 °C for 48 hours before any experiments were performed to allow elimination of SV40 expression. All in vitro experiments were conducted with cells at 60%–80% confluence.

For testing effects of the EA5 mouse monoclonal antibody (MedImmune, Inc) on SKOV3ip1 and HeyA8 ovarian cancer cells or murine endothelial cells growing in monolayer culture, various concentrations of the antibody were added to cells at 60% confluence. At various time points after addition of antibody, supernatant was collected for analyzing secreted vascular endothelial growth factor (VEGF), and cells were harvested and lysed, as described in the following section. Cells exposed to identical concentrations of murine IgG (clone 17, MedImmune, Inc) were used for controls. For analysis of effects of EA5 on Src and VEGF, additional controls included treatment of SKOV3ip1 cells with the Src inhibitor PP2 or its inactive form PP3 (Calbiochem, La Jolla, CA) or the protein tyrosine phosphatase (PTPase) inhibitor pervanadate (Sigma Chemical Co, St Louis, MO), with or without one-time EA5 treatment.

Preparation of Cell and Tumor Lysates

Lysates of cultured cells were prepared by washing cells with PBS and then incubating them in modified RIPA buffer (50 mM Tris, 150 mM NaCl, 1% Triton X-100, 0.5% deoxycholate) with the addition of 25 μg/mL leupeptin, 10 μg/mL aprotinin, 2 mM EDTA, and 1 mM sodium orthovanadate (Sigma) for 10 minutes at 4 °C. Cells were then removed from plates by scraping and centrifuged at 11 000*g* for 20 minutes at 4 °C. The supernatant was stored at −80 °C. Lysates were prepared from tumors that had been resected from mice at the conclusion of therapy experiments (see below), snap frozen in liquid nitrogen immediately after removal, and stored at −80 °C. A portion of the tissue (~50–100 mm^3) that was confirmed (by staining with hematoxylin and eosin) to contain tumor was incubated on ice in RIPA lysis buffer with 4× protease inhibitors (listed above) for 2 hours, homogenized with a mortar and pestle, and centrifuged at 11 000*g* for 20 minutes at 4 °C, and the supernatant was stored at −80 °C.

Immunoblot and Immunoprecipitation Analysis

Protein concentrations of lysates were determined using a BCA Protein Assay Reagent kit (Pierce Biotechnology, Rockford, IL). Lysates (25–50 μg protein) were separated on 10% sodium dodecyl sulfate–polyacrylamide gels. Proteins were transferred to a nitrocellulose membrane by semidry electrophoresis (Bio-Rad Laboratories, Hercules, CA), and the membranes were incubated overnight at 4 °C with primary antibody (mouse anti-human/mouse EphA2 monoclonal antibody [clone D7, Upstate, Lake Placid, NY], mouse anti-human VEGF monoclonal antibody [Upstate], mouse anti-human/mouse v-Src monoclonal antibody [Calbiochem], rabbit anti-human/mouse phosphorylated-Src^{Y419} monoclonal antibody [Cell Signaling, Danvers, MA], or mouse anti-human PTP-Basophil monoclonal antibody [FAP-1, Calbiochem]). Of note, the anti-EphA2 antibody recognizes both murine and human EphA2 and was used for immunoblot analysis of both ovarian cancer cells and murine endothelial cells, as per the manufacturer. Antibody binding was detected by incubating blots with 1 μg/mL horseradish peroxidase (HRP)–conjugated horse anti-mouse IgG or horse anti-rabbit IgG (Amersham, Piscataway, NJ). HRP was visualized by use of an enhanced chemiluminescence detection kit (Pierce). Equal loading and transfer were confirmed by probing the blots for β-actin (using 0.1 μg/mL of anti–β-actin primary antibody; Sigma). Band intensity was analyzed with Scion Image software (National Institutes of Health, Bethesda, MD), using β-actin as a control for each sample. For each individual lane, band intensity relative to its own actin control is presented in bar graph form below each immunoblot.

For immunoprecipitation studies, 500 μg of cell lysate was incubated with 6 μL of primary antibody (anti-pY [Upstate], anti-EphA2 [Upstate], or anti-Src [monoclonal antibody 327, Oncogene Sciences, Manhasset, NY]) for 30 minutes at 4 °C. Protein A sepharose beads (60 μL of a 1 : 1 dilution in PBS) were then added, and the mixture was incubated for 30 minutes at 4 °C. Laemmli buffer was added to dislodge complexes from beads, and beads were separated by centrifugation at 3500*g* for 5 minutes at 4 °C. The supernatants were then used for immunoblot analysis as described above with the appropriate antibodies.

Cell Viability Assay

HeyA8 cells (2×10^3) were plated in each well of a 96-well plate. Three wells were used for each experimental condition.

Twenty-four hours after plating, the medium was replaced with serum-containing growth media (RPMI-1640 supplemented with 15% FBS and 0.1% gentamycin sulfate) containing 10 μg/mL of EA5 or of the nonspecific mouse IgG clone I7 (MedImmune, Inc). At various times after antibody exposure, growth was assessed by adding 50 μL of 0.15% 3-(4,5-dimethylthiazol-2-yl)-2,5-diphenyl tetrazolium bromide (MTT) (Sigma) to each well. After incubation for 2 hours at 37 °C, the medium was removed, and cells were reconstituted in 100 μL of dimethyl sulfoxide (Sigma). The plate was shaken briefly to mix the samples, and the absorbance at 570 nm was recorded using a FALCON microplate reader (Becton Dickinson Labware, Franklin Lakes, NJ). Each data point was obtained by calculating the average of the three duplicate wells for each condition. In some experiments, cells were exposed to 10 μg/mL EA5 or IgG for 24 hours, and then increasing concentrations of docetaxel were added. The number of viable cells was assessed by MTT assay 5 days later. The concentration of docetaxel required for 50% inhibition of cell growth (IC_{50}) was determined by calculating the mean optical density (OD) at 570 nm ([max OD − min OD]/2 + min OD) and finding the docetaxel concentration at which this OD reading intersected the dose–response curve.

Orthotopic In Vivo Model and Tissue Processing

Female athymic nude mice (NCr-*nu*) were purchased from the National Cancer Institute—Frederick Cancer Research and Development Center (Frederick, MD) and housed in specific pathogen–free conditions. They were cared for in accordance with guidelines set forth by the American Association for Accreditation of Laboratory Animal Care and the US Public Health Service Policy on Human Care and Use of Laboratory Animals. All mouse studies were approved and supervised by the M. D. Anderson Cancer Center Institutional Animal Care and Use Committee.

For in vivo injection, cells were treated with trypsin to remove them from culture plates and centrifuged at 110*g* for 7 minutes at 4 °C, washed twice in PBS, and reconstituted in Hanks' balanced salt solution (Gibco, Carlsbad, CA) at a concentration of 5×10^6 cells/mL (SKOV3ip1 and HeyA8MDR) or 1.25×10^6 cells/mL (HeyA8) for 200 μL intraperitoneal injections. For analysis of short-term effects of treatment, mice (n = 2–3 per group) with intraperitoneal HeyA8 tumors (established tumors) that were palpable (i.e., 17 days after cell injection) were treated with IgG, EA5, paclitaxel, or combination therapy, as described for each experiment. For long-term experiments to assess tumor growth, therapy began 1 week after injection of cells (same number of cells as for short-term experiments). Mice were divided into four treatment groups (n = 10 mice per group): 1) control IgG, 2) EA5 anti-EphA2 antibody, 3) paclitaxel plus control IgG, or 4) paclitaxel plus EA5. Antibodies were diluted in PBS and injected intraperitoneally twice per week, at a dose of 10 mg/kg, in a volume of 180–220 μL (depending on mouse weight). Paclitaxel was diluted in PBS and injected intraperitoneally once a week, at a dose of 100 μg, in 200 μL. Mice were monitored for adverse effects, and tumors were harvested after mice were sacrificed by cervical dislocation, following 3–4 weeks of therapy. If any mouse in any group began to appear moribund or any tumor-bearing mouse was found dead from tumor burden, all mice in the entire experiment were killed together. Mouse weight, tumor weight, number of nodules, and distribution of tumor were recorded. Tissue samples were snap frozen for lysate preparation as described above, fixed in formalin for paraffin embedding, and frozen in optimal cutting temperature (OCT) media for preparation of frozen slides. Frozen tissues in OCT were cut into 8-μm sections, mounted on positive-charged slides, and air dried for 30 minutes. Additional survival experiments were performed in which treatment was initiated 7 days after cell injection and followed the same schedule as above. An additional survival experiment was conducted in mice with established HeyA8 tumors, in which therapy was initiated 17 days after cell injection, rather than 7 days after cell injection. The only endpoint of these experiments was the date of death. This date was recorded as the day before a mouse was found dead or on the day a mouse was killed. Survival experiments were terminated at 100 days or, in the case of SKOV3ip1, at 150 days so that the median survival time could be reached. The remaining mice were then killed, and the presence and weight of any tumor recorded.

Immunohistochemistry

Immunohistochemical analysis of EphA2, VEGF, and bFGF was conducted on established tumors from mice that were treated by intraperitoneal injection with two doses (on days 1 and 4) of EA5 at 10 μg/mL in 200 μL. Mice were killed on days 1, 4, 5, and 7 (three mice each day), and the tumors were harvested for analysis. Immunohistochemical analysis of PCNA and CD31 was conducted on tumors collected at the conclusion of 3–4 weeks of therapy. Formalin-fixed, paraffin-embedded tissue samples (used for analysis of all antigens except CD31) were cut into 8-μm sections and washed sequentially in xylene, 100% ethanol, 95% ethanol, 80% ethanol, and PBS. Antigen retrieval was then performed by heating slides in a steam cooker for 10 minutes in 0.2 *M* Tris buffer, pH 9.0 (for EphA2); microwave heating slides for 5 minutes in 0.1 *M* citrate buffer, pH 6.0 (for PCNA); and incubating slides in 0.5% pepsin at 37 °C for 20 minutes (for VEGF and bFGF). CD31 was analyzed in freshly cut (8 μm) OCT-embedded tissue frozen in liquid nitrogen. These slides were fixed in cold acetone for 10 minutes and did not require antigen retrieval. Endogenous peroxide was blocked by treating slides with 3% H_2O_2 in methanol for 5 minutes. After two washes in PBS, slides were blocked with 5% normal horse serum and 1% normal goat serum in PBS (blocking solution) for 15 minutes at room temperature and then incubated with primary antibody to CD31 (PECAM-1, rat IgG, Pharmingen, San Diego, CA), PCNA (PC-10, mouse IgG, DakoCytomation, Carpinteria, CA), VEGF (rabbit IgG, Santa Cruz Biotechnology, Santa Cruz, CA), or bFGF (rabbit IgG, Sigma) in blocking solution overnight at 4 °C. After two washes with PBS, the appropriate HRP-conjugated secondary antibody in blocking solution was added for 1 hour at room temperature. Slides were stained with DAB substrate (Phoenix Biotechnologies, Huntsville, AL) for 5 minutes, washed, and counterstained with Gil No.3 hematoxylin (Sigma) for 20 seconds. A slightly different procedure was used for immunohistochemical analysis of EphA2. After the slides were treated to block endogenous peroxidase activity, they were incubated with 0.13 μg/mL mouse IgG Fc blocker (Jackson Laboratory, Bar Harbor, ME) for 2 hours before incubation with the primary antibody (EA5 clone, MedImmune, Inc). For EphA2 staining, 0.5% blocking reagent was used (from the TSA biotin system kit, PerkinElmer Applied Biosystems, Boston, MA), and to visualize antibody binding it was necessary to enhance

the signal by treating slides with 1.5 μg/mL biotinylated horse anti-mouse antibody (Vector Laboratories, Burlingame, CA) for 10 minutes at room temperature, followed by 0.75 μg/mL streptavidin–HRP (DakoCytomation, Carpinteria, CA) for 30 minutes. After PBS wash, DAB was added for 7 minutes, and slides were counterstained with hematoxylin and mounted under coverslips.

Terminal Deoxynucleotidyl Transferase Biotin–Deoxyuridine Triphosphate Nick-End Labeling–CD31 Colocalization Studies

Terminal deoxynucleotidyl transferase biotin–deoxyuridine triphosphate nick-end labeling (TUNEL)–CD31 staining was conducted on established tumors from short-term therapy experiment described above treated with two doses (days 1 and 4) of 10 μg/mL EA5 and collected from mice killed on days 1, 4, 5, and 7 (three mice per day). Tissue was placed immediately in OCT media and frozen rapidly in liquid nitrogen *(38,39)*. Slides were fixed in acetone for 5 minutes, in acetone : chloroform (vol/vol) for 5 minutes, and then in acetone for 5 minutes. They were then washed with PBS, blocked with 10% fish gelatin in phosphate-buffered saline (PBS) for 20 minutes, and exposed to 1 : 400 rat anti-CD31 antibody (PECAM-1, rat IgG, Pharmingen) in blocking solution for 18 hours at 4 °C followed by 1 : 200 anti-rat secondary antibody labeled with Texas Red (Molecular Probes, Eugene, OR). Slides were washed in PBS, fixed again in 4% paraformaldehyde in PBS, washed twice in PBS, and incubated with 0.2% Triton X-100 in PBS for 15 minutes. After two more washes in PBS, slides were incubated for 10 minutes with the equilibration buffer provided in the TUNEL detection kit (Promega, Madison, WI). Equilibration buffer was removed, and reaction buffer (consisting of kit-provided equilibration buffer, fluorescein-12-dUTP, and terminal deoxynucleotidyl transferase [TdT] enzyme) was then added. After a 1-hour incubation at 37 °C in the dark, the reaction was stopped by addition of the provided 2× standard saline citrate (SSC) buffer for 15 minutes. Excess dUTP was removed by washing, and nuclei were stained with 1.0 μg/mL Hoescht (Molecular Probes, in PBS) for 10 minutes. Slides were covered with propylgallate and coverslips for microscopic evaluation. Microscopy was performed with a Zeiss AxioPlan 2 microscope, Hamamatsu ORCA-ER digital camera, and ImagePro software. The total number of CD31-positive cells (red staining), and apoptotic CD31-positive cells (red cells plus green nuclei) were counted. Controls included a slide exposed to only secondary antibodies, one in which reaction buffer did not contain TdT, and one subjected to DNA fragmentation (positive control).

In Situ Hybridization

VEGF mRNA levels were assessed in formalin-fixed, paraffin-embedded tissue from the short-term experiment on established tumors described above that had been sectioned and mounted on ProbeOn slides using the Microprobe manual system (Fisher Scientific, Pittsburgh, PA). Slides were deparaffinized and rehydrated as described above and subjected to enzymatic digestion with pepsin (Dako) for 20 minutes at 37 °C. Slides were incubated with a biotinylated VEGF probe with the sequence 5′-TGGTGATGTTGGACTCCTCAGTGGGCU-3′ (1 : 200 dilution in PBS), for 60 minutes at 45 °C. They were then washed three times, for 2 minutes each, in 2× SSC at 45 °C, incubated with alkaline phosphatase–labeled avidin (Dako) for 30 minutes at 45 °C, rinsed in 50 mM Tris–HCl buffer (pH 7.6), exposed to alkaline phosphatase enhancer (Biomeda Corp, Foster City, CA) for 1 minute, and finally incubated with Fast Red chromagen substrate (Research Genetics, Carlsbad, CA) for 30 minutes at 45 °C. Red staining indicates a positive reaction. Concurrent controls were performed. The negative control included all steps, with elimination of biotinylated probe from the hybridization reaction. The positive control used a poly$(dT)_{20}$ oligonucleotide, which provided both confirmation of mRNA integrity and a comparison group for analysis of stain intensity. All samples, including controls, were tested together in a single experimental run. For imaging analysis, regions at the periphery of the tumor, representing the areas of greatest staining, were compared between groups. Four photographs of each slide were taken. Ten areas of each photograph were selected at random, and the histogram output of mean staining intensity using the histogram tool in Adobe Photoshop was recorded as intensity of staining. Both the intensity of staining as given by histogram measurement and a "relative" score are given. For relative scoring, the absolute intensity measurement for the negative control is designated zero and the absolute intensity measurement for the positive control is designated 100, with relative intensity scores for experimental samples calculated based on these reference points.

Enzyme-Linked Immunosorbent Assays

We analyzed EA5 cross-reactivity to other Eph receptor isoforms, to define the specificity of the antibody. Maxisorp enzyme-linked immunosorbent assay (ELISA) plates were coated with EA5 antibody (50 μL per well of 5 μg/mL antibody) overnight at 4 °C. Plates were washed with PBS and then blocked with 2% bovine serum albumin, 0.1% Tween-20 in PBS. Recombinant biotinylated Eph receptors (EphA1, EphA2, EphA3, EphA4, EphA5, EphA6, EphA7, EphA8, EphB1, EphB2, EphB3, EphB4, and EphB6; R&D Systems, Minneapolis, MN) were then added to the plates, which were incubated for 1 hour at 37 °C. The plates were washed and exposed to 50 μL of neutravidin–HRP (Pierce) (1 : 2500) in blocking solution for 1 hour at 37 °C, washed in PBS, and incubated with 50 μL of KPL SureBlue TMB peroxidase (Kirkegaard & Perry Laboratories, Gaithersburg, MD) for 10 minutes. The reaction was stopped with 50 μL of 0.2 M H_2SO_4, and the plate was read at 450 nm. For ELISA to examine levels of secreted VEGF in the supernatant of treated cultured cells, the VEGF Quantikine kit from R&D Diagnostics (Minneapolis, MN) was used according to the manufacturer's instructions.

Reverse Transcription–Polymerase Chain Reaction

Total RNA was isolated and prepared from HeyA8 and SKOV3ip1 cells using the RNAeasy minikit (Qiagen, Valencia, CA) according to the manufacturer's instructions. Quantitative reverse transcription–polymerase chain reaction (RT–PCR) for EphA2 and EphA1 was performed using primer sets from Applied Biosciences. As described previously *(40)*, genes were amplified using a Gene Amp 5700 Sequence Detection System (PerkinElmer Applied Biosystems). The PCR cycling conditions were as follows: 50 °C for 10 minutes, followed by 40 cycles of 95 °C for 30 seconds, 60 °C for 1 minute, and 72 °C for1 minute. The relative quantity of EphA2 and EphA1 gene products were calculated

from the standard curve determined by amplification of the GAPDH gene, according to the manufacturer (User Bulletin 2, PerkinElmer Applied Biosystems). Each sample was assayed in triplicate, and the entire experiment was duplicated once to confirm results.

Statistical Methods

Continuous variables were compared with the Student's *t* test (between two groups) or analysis of variance (ANOVA; for all groups) if normally distributed and the Mann–Whitney rank sum test if distributions were nonparametric. To control for the effects of multiple comparisons (i.e., in experiments analyzing treatment with IgG, paclitaxel, EA5, or combination therapy), a Bonferroni adjustment was made; for this analysis, a P value $\leq .017$ was considered statistically significant. For in vivo therapy experiments, 10 mice in each group were used, as directed by a power analysis to detect a 50% reduction in tumor weight (beta error = 0.2). ANOVA for tumor weight and log of tumor weight was used to examine interactions between treatments. Survival curves were plotted by the method of Kaplan and Meier and tested for differences with the log-rank statistic. A $P<.05$ on two-tailed testing was considered statistically significant. All confidence intervals (CIs) are given at the 95% level.

Results

Effect of the Monoclonal Antibody EA5 on EphA2 Expression

We began by examining the dose and kinetics by which the agonistic antibody EA5 influenced EphA2 protein levels. HeyA8 or SKOV3ip1 ovarian cancer cells were exposed to varying concentrations of EA5 in vitro and subjected to immunoblot analysis of EphA2 after 2–7 days (Fig. 1, A). A dose-dependent reduction in levels of total EphA2 was observed, with 10 μg/mL resulting in strong reduction in EphA2 for at least 3 days. Levels returned to baseline by 7 days. The reduction in EphA2 levels was preceded by a rapid increase in phosphorylation of EphA2 (Fig. 1, B), consistent with the agonistic nature of the antibody.

To confirm that this antibody was targeting EphA2 specifically without cross-reacting to other Eph subtypes, we performed an ELISA analysis against recombinant biotinylated Eph receptors. The binding of EA5 was greatest for EphA2, with intermediate binding noted for EphA1 (data not shown). No binding was noted for any of the other receptors. The SKOV3ip1 and HeyA8 cell lines were examined for EphA1 expression by RT–PCR and found to be negative (data not shown).

We next sought to determine whether EA5 might trigger a similar reduction in EphA2 levels in vivo. To test the in vivo effects of EA5, nude mice bearing intraperitoneal HeyA8 tumors were injected intraperitoneally with a single dose of 5 or 10 mg/kg of EA5 or with an isotype-matched antibody as a negative control. One, 4, 5, and 7 days after injection, tumors were harvested and subjected to immunoblot and immunohistochemical analysis of EphA2 expression. Immunoblot analysis (Fig. 1, C) revealed a dose- and time-dependent effect of EA5 on the level of total EphA2, with reduction of at least 90% persisting for at least 7 days at the 10 mg/kg dose level in all mice tested (n = 8). Tumor tissue subjected to immunohistochemical analysis confirmed the effect of EA5 on EphA2 levels (Fig. 1, D). Therefore, a dose of 10 mg/kg twice per week was selected for subsequent long-term therapy experiments.

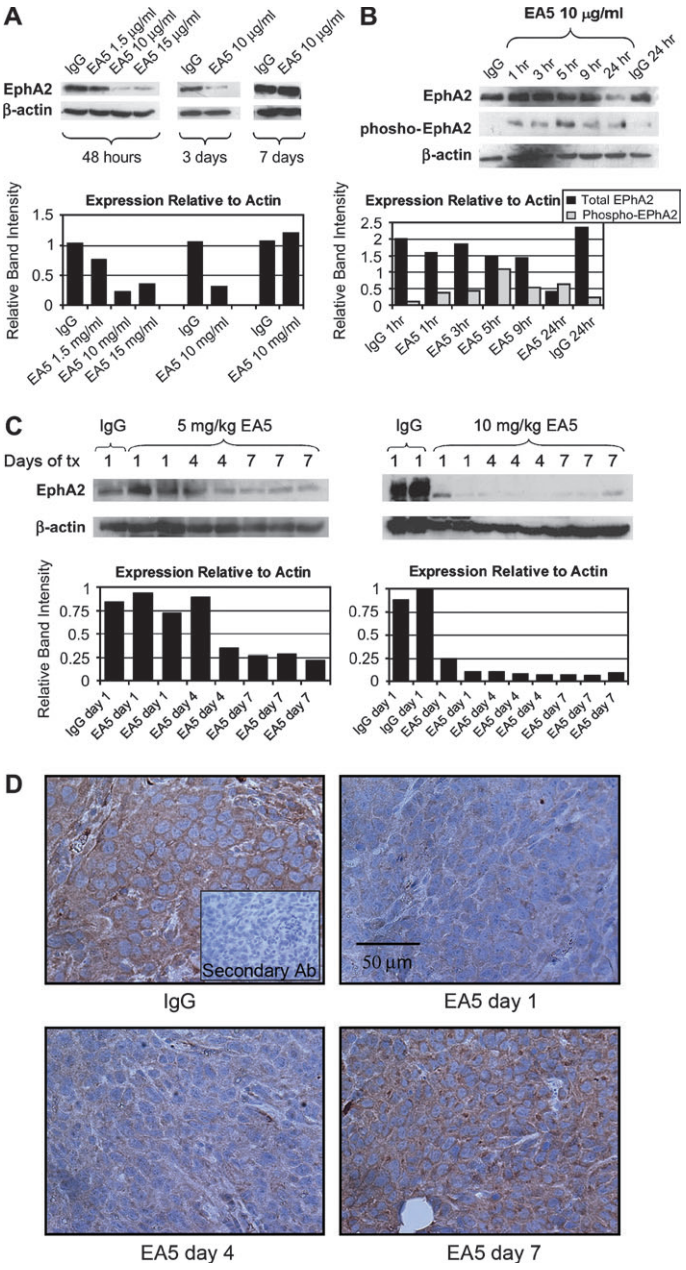

Fig. 1. Dose- and time-dependent reduction of EphA2 with EA5 treatment. **A**) HeyA8 ovarian cancer cells were exposed to increasing doses of the agonistic monoclonal antibody EA5 or isotype control IgG for varying times. Cell lysates were then subjected to immunoblot analysis of total EphA2. **B**) HeyA8 cells were exposed to 10 μg/mL of EA5 or to IgG for varying times, and separate cell lysate samples were analyzed for total EphA2 by immunoblotting or for phosphorylated EphA2 by immunoprecipitation with an antiphosphotyrosine antibody followed by immunoblotting for total EphA2. **C**) Mice (n = 8) bearing palpable intraperitoneal HeyA8 tumors (17 days after cell injection) were injected intraperitoneally with a single dose of EA5 (5 or 10 mg/kg) or IgG (10 mg/kg). Mice were killed and tumors were collected at 1, 4, or 7 days, and tumor lysates were analyzed by immunoblot analysis for EphA2. Each lane represents a separate mouse. In panels (**A**–**C**), the immunoblot is shown at the top and quantification of band intensity relative to β-actin intensity is shown below. Results were confirmed with a duplicated experiment. **D**) EphA2 expression in the tumors treated with 10 mg/kg EA5 (analyzed in panel **C**) was assessed by immunohistochemistry. **Inset** in IgG panel represents exposure of tissue to secondary antibody only, as a negative control.

Long-Term Therapy of Orthotopic Ovarian Tumors With EA5

To examine the potential therapeutic efficacy of EA5, we carried out several analyses using an orthotopic model of advanced ovarian cancer. The HeyA8 and SKOV3ip1 cell lines were used because they were derived from women with advanced, therapy-refractory ovarian cancer and represent the extremes of growth seen in human patients. We also used the HeyA8MDR cell line, a derivative of the parental HeyA8 cell line that is resistant to taxane and platinum compounds for in vivo long-term therapy studies. We analyzed this line because a common clinical problem in ovarian cancer is the scenario of chemotherapy-resistant cancer. Specifically, approximately 30% of tumors at initial presentation, and about 70% of tumors at the time of recurrence, are resistant to taxane–platinum chemotherapy *(41)*.

To simulate advanced disease, we initiated therapy 1 week after tumor cell injection, during which time cells are allowed to seed the peritoneum. Mice were assigned to one of four groups (n = 10 mice per group): 1) isotype-matched control (IgG), 10 mg/kg twice per week; 2) EA5, 10 mg/kg twice per week; 3) paclitaxel, 100 μg, once per week, plus control IgG; or 4) paclitaxel, 100 μg, once per week, plus EA5 [The combination therapy group was included based on overwhelming clinical evidence that drug combinations can provide additive or synergistic benefit with regard to objective patient responses or survival rates *(3)*.] For these studies, treatment was continued until control animals had clinically significant tumor burden and became moribund (generally ~3 weeks for HeyA8 and HeyA8MDR and ~4 weeks for SKOV3ip1), at which time all mice in an experiment were killed together. Prolonged EA5 therapy led to a reduction in the growth of HeyA8, SKOV3ip1, and HeyA8MDR tumors (Fig. 2). For the HeyA8 cell line, treatment with EA5 alone led to a 45% (95% CI = 20% to 70%) reduction in tumor weight compared with that in control mice (Fig. 2, A, $P = .01$). For the SKOV3ip1 cell line (Fig. 2, B), EA5 treatment reduced tumor weight by 31% (95% CI = −9% to 71%, $P = .27$). In both cell lines, the efficacy of EA5 was comparable to that of paclitaxel alone. With the HeyA8MDR cell line (Fig. 2, C), treatment with EA5 alone was not superior to control treatment (mean tumor weight = 2.17 g [95% CI = 1.47 to 2.88 g] versus 1.88 g [95% CI = 1.45 to 2.31 g], $P = .77$). Not surprisingly, paclitaxel alone did not lead to a reduction in tumor weight (2.17 g [95% CI = 1.47 to 2.88 g] versus 1.99 g [95% CI = 1.44 to 2.53 g], $P = .88$). However, the combination of EA5 and paclitaxel was superior to paclitaxel alone, with a 47% (95% CI = 24% to 72%) reduction in tumor weight ($P = .009$).

Combination therapy with paclitaxel and EA5 in mice with HeyA8 tumors resulted in an 80% (95% CI = 68% to 91%) reduction in tumor weight compared to treatment with paclitaxel/IgG ($P<.001$). For SKOV3ip1 tumors, combination therapy with paclitaxel/EA5 was also superior to that with paclitaxel/control IgG, with a 77% (95% CI = 63% to 91%) reduction in tumor weight ($P = .009$). No statistically significant interaction between EA5 and paclitaxel was evident in ANOVA on tumor weight, suggesting that the combination had additive but not synergistic effects.

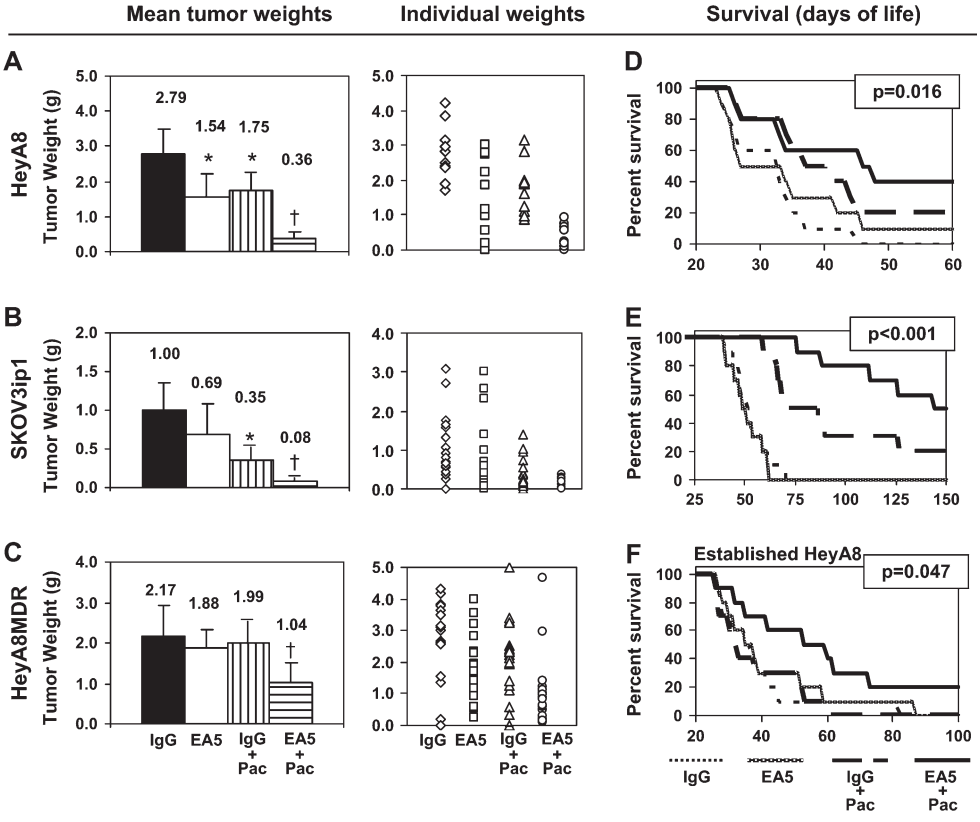

Fig. 2. Tumor size and survival of orthotopic tumor–bearing mice treated with EA5 alone or in combination with paclitaxel. **A**–**C**) Mice (n = 10 per treatment group, 40 per cell line) injected with HeyA8 (**A**), SKOV3ip1 (**B**), or HeyA8MDR (**C**) ovarian cancer cells were treated by intraperitoneal injection with IgG (10 mg/kg twice per week), EA5 (10 mg/kg twice per week), IgG plus paclitaxel (Pac; 100 μg once per week), or EA5 plus paclitaxel. When control mice were moribund (3–4 weeks after cell injection), mice in all groups were killed, tumors excised, and tumor weights recorded. Mean weights with 95% confidence intervals and individual weights from each experiment are shown. Reported weights for SKOV3ip1 and HeyA8MDR tumors represent data from two independent experiments. Statistical analysis (Student's *t* test if tumor weight was normally distributed, Mann–Whitney rank sum test if test for normality failed) was performed on the combined data from these two trials, the conclusions of which were the same as when each trial was analyzed individually. *, $P<.05$ compared with IgG treatment; †, $P<.05$ compared with paclitaxel plus IgG treatment; see text for exact *P* values. **D**–**E**) Separate survival experiments were performed in mice carrying HeyA8 (**D**) and SKOV3ip1 (**E**) orthotopic tumors created as described above. Mice (n = 10 per group) were treated with EA5, IgG, paclitaxel, or EA5 plus paclitaxel in the same schedule as above until individually moribund, when they were killed and days of life recorded. Survival differences among treatment groups were analyzed with the log-rank statistic. **F**) Survival experiment in mice bearing HeyA8 tumors, created by intraperitoneal injection of cells, with therapy initiated 17 days after injection when tumors are palpable.

Table 1. Characteristics of tumors after treatment with EA5 with and without paclitaxel*

Cell line	Experimental group	No. of nodules, mean (95% CI)	P†	P‡
HeyA8	IgG	3.0 (2.3 to 3.7)	–	.016
	EA5	1.6 (1.2 to 2.0)	.003	.36
	IgG + paclitaxel	2.1 (1.7 to 2.5)	.032	.51
	EA5 + paclitaxel	1.9 (1.4 to 2.4)	.016	–
SKOV3ip1	IgG	20.4 (14.1 to 26.1)	–	<.001
	EA5	4.6 (2.6 to 6.6)	<.01	.005
	IgG + paclitaxel	3.2 (2.1 to 4.3)	<.01	.002
	EA5 + paclitaxel	0.9 (0.44 to 1.4)	<.001	–

*Mice (n = 10 per group) injected intraperitoneally with HeyA8 or SKOV3ip1 ovarian cancer cells were treated for 4 weeks with control IgG antibody, the EphA2-agonistic monoclonal antibody EA5, paclitaxel with IgG, or paclitaxel with EA5 as described in Methods. Mice were then killed, and the number of nodules formed was determined. CI = confidence interval.

†*P* values determined for comparison with IgG alone by Student's *t* test.

‡*P* values determined for comparison with EA5 + paclitaxel group by Student's *t* test.

In addition to comparing tumor weight among the treatment groups, we compared the numbers of nodules present at the conclusion of treatment (Table 1). In the HeyA8 model, treatment with EA5, paclitaxel, or combination therapy led to a statistically significant reduction in the number of nodules compared with that in IgG-treated controls. Combination therapy was not statistically superior to single-agent therapy. In the SKOV3ip1 model, which typically grows in a multifocal carcinomatosis pattern, all three treatments also led to a statistically significant reduction in the number of nodules. Furthermore, combination therapy further reduced the number of nodules compared with either EA5 or paclitaxel alone.

Survival in Long-Term EA5 Therapy of Ovarian Cancer

Based on the encouraging results with regard to inhibition of in vivo tumor growth, we next examined the effects of EA5 therapy on survival. In these experiments, therapy was again initiated 1 week after tumor cell injection and continued with weekly (paclitaxel) and twice weekly (IgG and EA5) treatments as described for the tumor growth experiments until each animal became moribund. In mice bearing tumors derived from the HeyA8 cell line, survival was not prolonged in mice treated with EA5 alone (median survival = 27 days) compared with that in control mice (median survival = 32 days, Fig. 2, D). Paclitaxel led to a modest, but not statistically significant, improvement in survival (median = 37 days) as compared with control mice. The combination of EA5 and paclitaxel yielded a statistically significant survival advantage over paclitaxel alone (median survival = 46 days, $P = .016$). This HeyA8 cell line experiment was continued for 100 days, with the same number of mice alive at 100 days as were alive at 60 days (n = 4 for paclitaxel/EA5 and n = 2 for paclitaxel/IgG). None of these mice had residual tumor at necropsy.

Mice bearing SKOV3ip1 tumors also showed a survival benefit with combination therapy (Fig. 2, E). EA5 alone did not improve survival, with a median survival of 49 days for EA5 and 51 days for control mice. Paclitaxel statistically significantly prolonged survival, with a median survival of 69 days ($P<.01$). The combination of EA5 and paclitaxel was substantially superior to paclitaxel alone, with a median survival of 144 days ($P<.001$). After 150 days, the remaining living mice (two in the paclitaxel group and five in the combination group) were killed. One of the paclitaxel-treated mice had substantial tumor burden (1.45 g in three nodules), and the other was tumor free. Two of the EA5/paclitaxel-treated mice each had a small single-site tumor (0.37 and 0.66 g), and three had no visible tumor.

When first diagnosed, the majority of ovarian cancer patients will undergo primary debulking surgery and therefore have minimal residual disease when they start initial chemotherapy. However, women with recurrent or drug-resistant disease will usually have varying degrees of tumor burden when considering treatment options. Therefore, we examined the effects of initiating EphA2-targeted therapy in mice with an existing HeyA8 tumor burden. Therapy was initiated 17 days after HeyA8 cell injection, when mice had palpable tumors in the range of 0.5–0.75 cm^3. Treatment was continued until death, and days of life were recorded (Fig. 2, F). Neither EA5 nor paclitaxel therapy alone prolonged life compared with that in control mice, with a median survival of 31 and 35 days, respectively, compared with 35 days for control IgG. However, the combination of EA5 and paclitaxel resulted in statistically significant prolongation of survival, with a median survival of 53 days ($P = .047$).

Antiproliferative Effects of EA5

To determine whether EA5 has direct antiproliferative effects on tumor cells, HeyA8 cells were treated in vitro with either EA5 (10 μg/mL) or a control IgG antibody, and the number of viable cells was assessed by MTT assay. There was no difference in viability of cells treated with EA5 and IgG at any time point tested (Fig. 3, A). In similar experiments with EA5 in combination with docetaxel, we observed no difference in the calculated IC_{50} when compared with IgG (Fig. 3, B). That is, EA5 did not sensitize HeyA8 cells to docetaxel in vitro. (Docetaxel was used in place of paclitaxel in these experiments because the diluent for this taxane is more compatible with physiologic growth media than that of paclitaxel).

Although proliferation was not affected in vitro, the in vivo studies clearly showed reduced tumor growth in treated mice. Therefore, we examined the effects of EA5, paclitaxel, and combination therapy on proliferation in vivo by carrying out immunohistochemistry analysis of PCNA in tumors from treated mice (Fig. 3, C). Whereas in tumors treated with IgG, 51.5% (95% CI = 48.7% to 54.4%) of the nuclei were PCNA positive, only 21.5% (95% CI = 15.5% to 27.6%) and 24.9% (95% CI = 21.7% to 28.0%) of cells were PCNA positive in tumors treated with EA5 or paclitaxel, respectively ($P<.001$ for both). Moreover, tumors that had been treated with combination therapy showed an even greater reduction in percentage of PCNA-positive cells, 12.9% (95% CI = 10.2% to 15.7%), a statistically significant reduction compared with either treatment alone ($P<.001$). These data suggest that the observed in vivo effects of EA5 therapy on proliferation were likely indirect.

Antiangiogenic Effects of EA5 Therapy

One mechanism by which a compound may decrease tumor cell proliferation in vivo without having direct cellular antiproliferative effects is through indirect effects on the vasculature. Previous evidence for a role of EphA2 in VEGF-mediated angiogenesis *(42–44)* led us to consider the possibility that a reduction in EphA2

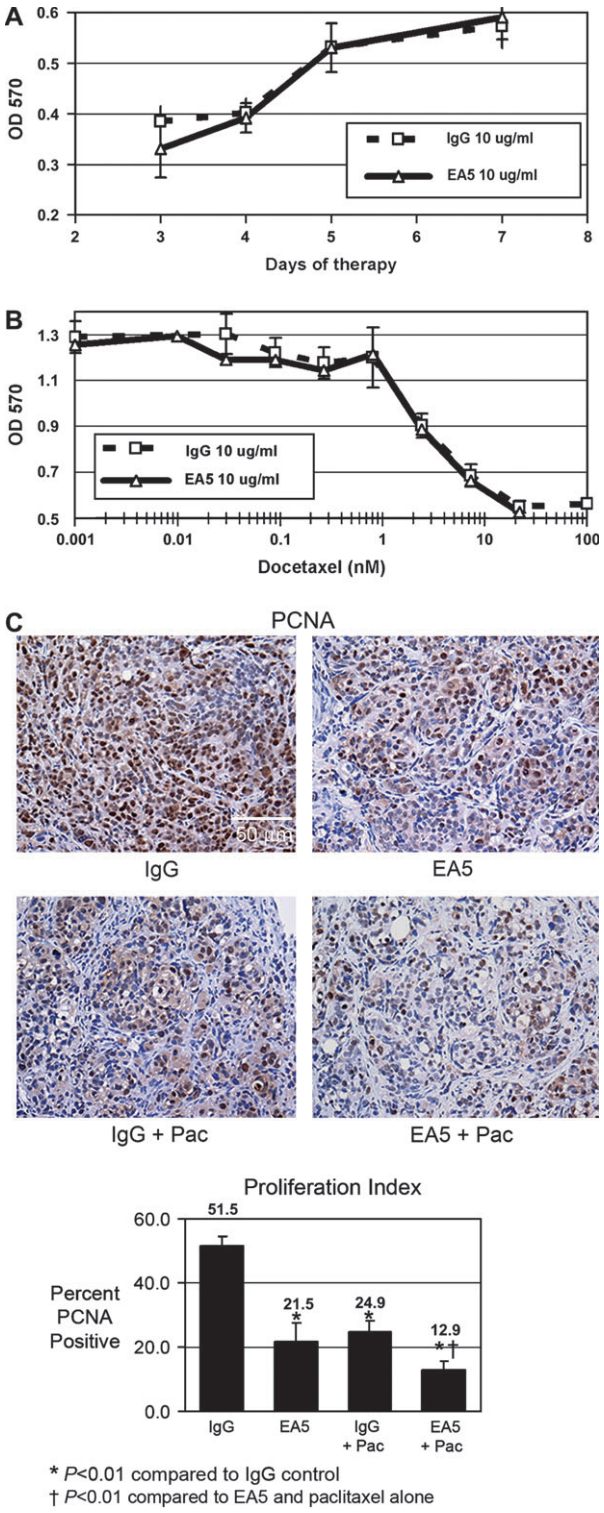

Fig. 3. Effects of EA5 therapy on viability and proliferation of ovarian cancer cells. **A**) Viability of HeyA8 ovarian cancer cells was assessed by 3-(4,5-dimethylthiazol-2-yl)-2,5-diphenyl tetrazolium bromide (MTT) assay at increasing time points after cells were treated with a single dose of EA5 or IgG (10 μg/mL). Results were confirmed with duplicate experiments. **Error bars** indicate 95% confidence intervals (CIs). **B**) Viability of HeyA8 ovarian cancer cells was assessed by MTT 5 days after exposure to increasing concentrations of docetaxel, which was added 24 hours after incubation with 10 μg/mL EA5 or IgG began. **Error bars** indicate 95% CIs. **C**) SKOV3ip1 tumors collected at the conclusion of the experiments in Fig. 2, A and B, were stained for proliferating cell nuclear antigen (PCNA). Representative sections (final magnification = ×100) are shown, with mean percentages (and 95% CIs) of PCNA-positive cells. PCNA positivity was analyzed in four fields per slide and at least three slides per group (all from different mice).

levels may have an antiangiogenic effect. We therefore assessed microvessel density in these tumors by staining for CD31 (Fig. 4, A). The mean number of vessels per field in tumors from control (IgG treated) mice was 14.9 (95% CI = 13.5 to 16.3), whereas in tumors treated with EA5 there were an average of 8.1 vessels per field (95% CI = 7.0 to 9.2, $P<.001$). Microvessel density in tumors in mice treated with paclitaxel/IgG was 14.1 (95% CI = 12.2 to 16.0) and that in mice treated with combination EA5/paclitaxel was 6.1 (95% CI = 5.0 to 7.1, $P<.001$). This outcome did not reflect a generalized decrease in tumor growth, because the microvessel density of paclitaxel-treated tumors was not statistically significantly different from controls, despite the reduced tumor weight seen with paclitaxel therapy.

To examine the rapid effect of EphA2 reduction on tumor-associated endothelial cells, mice bearing intraperitoneal tumors were treated with two doses of EA5 and examined for endothelial cell apoptosis by TUNEL analysis, with CD31 colocalization (Fig. 4, B). Tumors from mice treated with IgG had prominent vasculature and no apoptotic CD31-positive cells. In mice from which tumors were taken 24 hours after treatment with a single dose of EA5, a small percentage of CD31-positive cells (0.7%, 95% CI = 0.0% to 1.4%) were apoptotic. Similar percentages were seen in tumor samples taken immediately before the second EA5 dose (i.e., 96 hours after the first dose; data not shown). However, 48 hours after the second dose, a statistically significant rise in the percentage of apoptotic CD31-positive cells (to 5.8%; 95% CI = 2.9% to 8.6%, $P = .036$) was noted.

EphA2 is expressed on both tumor cells and angiogenic blood vessels within the tumor microenvironment *(25,29,30,33,45,46)*. To determine if a direct effect of EA5 antibody on mouse endothelial cell EphA2 expression could explain its observed antivascular effects in vivo, we investigated whether EphA2 is expressed on murine endothelial cells and if EA5 treatment affects murine EphA2 expression. Murine endothelial cells isolated from the mesentery or ovary of the immortomouse *(37)* were exposed to 10 μg/mL of EA5 and subjected to western blot analysis for total EphA2 (Fig. 4, C). Antibody treatment for up to 72 hours did not lead to a reduction in EphA2 expression at any time point in either cell line compared with that in IgG-treated cells.

Effect of EA5 on Angiogenic Cytokines

The observation that EA5 does not affect murine EphA2 expression but does inhibit host angiogenesis led us to hypothesize that EA5 may act on the tumor cells themselves to block the production of angiogenesis-promoting factors, such as VEGF. Therefore, we analyzed tumor VEGF expression in mice treated with EA5. A slight reduction in VEGF protein expression was seen 24 hours after the first dose of EA5, and a strong reduction was noted 48 hours after a second dose (Fig. 5, A). The effects of EA5 on VEGF expression, like those on EphA2 expression (Fig. 1, D), were reversible, in that tumors collected 7 days after the second dose showed prominent VEGF expression.

To determine if the reduction in VEGF protein was mediated through a reduction in VEGF mRNA, the tumor tissues were subjected to in situ hybridization using VEGF primers (Fig. 5, B). VEGF mRNA levels were high in IgG-treated tissue (intensity score of 89.5, 95% CI = 82.3 to 96.6), approaching that of the Poly(dT)–positive control (assigned intensity score of 100). Twenty-four hours after treatment with the second dose of EA5, there was a modest reduction in intensity score, to 73.5

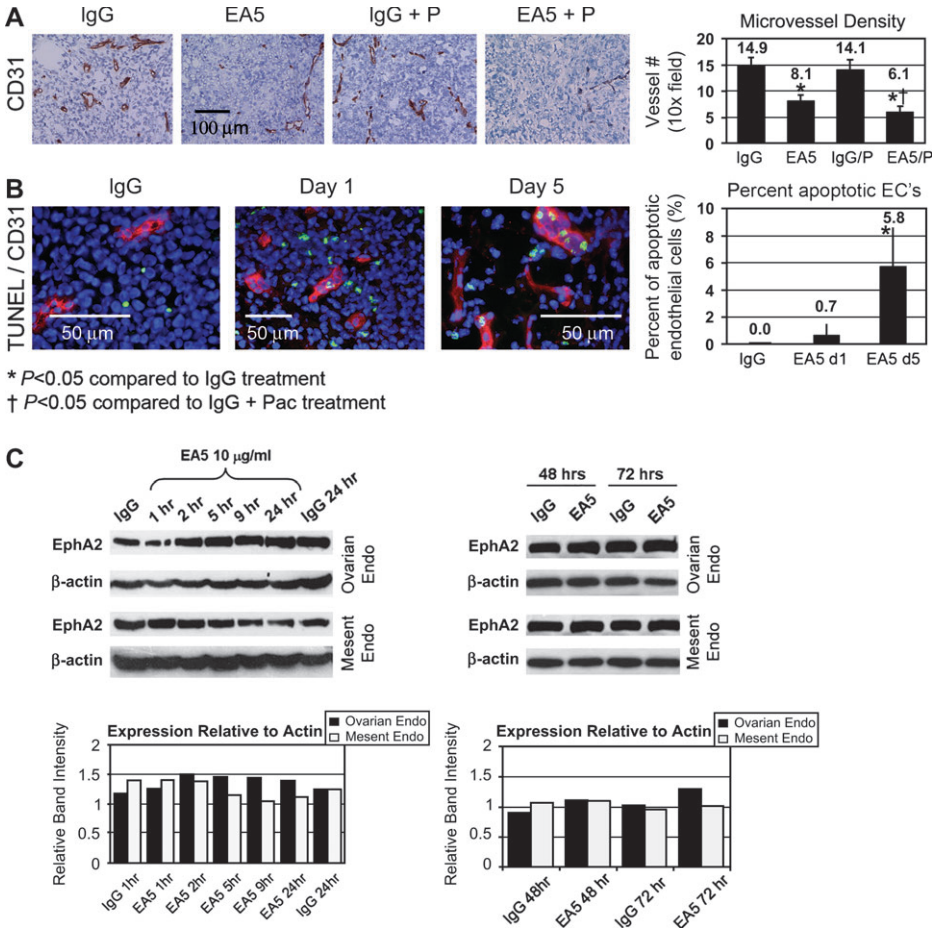

Fig. 4. Antivascular effects of EA5. **A**) Tumors collected at the conclusion of therapy experiments (Fig. 1, A and B) were subjected to immunohistochemistry for CD31 to allow identification of endothelial cells. A lumen with positive CD31 staining was counted as a single microvessel. Representative sections from each treatment group (P = paclitaxel) are shown (final magnification = ×100), with the mean number of vessels per field (with 95% confidence intervals) indicated at the right. Five fields per slide, and at least three slides per treatment group, were examined. Microvessel density was compared among treatment groups with student's *t* test and analysis of variance. **B**) Mice bearing palpable HeyA8 tumors were treated with two doses (on days 0 and 3) of 10 mg/kg EA5 injected intraperitoneally. Frozen tumor sections were subject to immunofluorescence analysis of CD31 (**red**), followed by terminal deoxynucleotidyl transferase biotin–deoxyuridine triphosphate nick-end labeling (TUNEL) assay to identify apoptotic cells (**green**) (final magnification = ×200). Representative micrographs are shown, with quantification on the right (the average of 10 frames for each group). **C**) Murine endothelial cells extracted from the ovary or mesentery of the immortomouse *(37)* and established in culture were treated with EA5 as a single-dose administration of 10 μg/mL in cultured cells at 60% confluence and subjected to immunoblotting for total EphA2. **Graphs at bottom** show band intensity relative to β-actin loading control.

(95% CI = 65.6 to 81.5, $P = 0.11$), and 4 days after treatment there was a statistically significant reduction to 62.2 (95% CI = 58.0 to 66.4, $P = .01$, compared with IgG-treated controls).

We also examined EA5 effects on expression of bFGF. Antibody treatment did not decrease bFGF expression in tumors (Fig. 5, C). Combined therapy had similar effects on VEGF and bFGF levels as treatment with EA5 alone, and no treatment effect was noted with paclitaxel/control IgG, supporting the conclusion that effects are mediated by EA5 treatment. Decreased VEGF expression in tumors was also noted on western blots of the tumor lysate (Supplementary Fig. 1, available at: http://jnci cancerspectrum.oxfordjournals.org/jnci/content/vol98/issue21/). Together, these results relate the agonistic antibody-mediated degradation of EphA2 with decreased transcription of VEGF, suggesting a possible mechanism for the observed decrease in microvessel density with EA5 treatment.

Mechanisms Linking EphA2 Reduction to Decreased VEGF Expression

To investigate potential mechanisms by which EphA2 reduction with this agonistic antibody inhibits VEGF transcription and subsequent expression and angiogenesis, we examined the effects of EA5 treatment on phosphorylation of Src, which is implicated in tumor angiogenesis and, specifically, expression of VEGF *(47–49)*. Src was rapidly dephosphorylated on Y419 in SKOV3ip1 cells within 10 minutes of treatment with EA5 at 10 μg/mL, coincident with the observed rapid phosphorylation of EphA2 with EA5 treatment (Fig. 6, A). After addition of EA5 to cells, VEGF levels showed a detectable decrease at 1 hour, with a profound decrease noted at 12 hours later (Fig. 6, A).

ELISA analysis of VEGF protein was carried out to test secretion of VEGF by cells after EA5 treatment. This analysis revealed that VEGF protein levels at 24 hours following EA5 treatment of SKOV3ip1 cells (mean = 179 pg/mL, 95% CI = 136 to 222 pg/mL) were 41% less than those in cells treated with control IgG (302 pg/mL, 95% CI = 263 to 342 pg/mL; $P = .02$). VEGF levels were also decreased in response to the Src family selective inhibitor PP2, but not its inactive form PP3 (Fig. 6, B). By ELISA, there was a 46% decrease in VEGF levels following treatment with PP2 (207 pg/mL, 95% CI = 175 to 239 pg/mL) relative to levels in PP3-treated cells (384 pg/mL, 95% CI = 331 to 438 pg/mL) and PBS-treated cells (338 pg/mL, 95% CI = 345 to 430 pg/mL; $P = .028$). Treatment with pervanadate, an inhibitor of PTPase, blocked EA5-mediated Src dephosphorylation (Fig. 6, C). Similar results were obtained with phenylarsine oxide, another PTPase inhibitor (data not shown).

To investigate whether dephosphorylation of Src occurs specifically in Src–EphA2 complexes, as opposed to in Src not associated with EphA2, we performed coimmunoprecipitation experiments. In the absence of EA5, EphA2 was present in Src immunoprecipitates and Src was detected in EphA2 immunoprecipitates (Fig. 6, D). Treatment of SKOV3ip1 cells with EA5 resulted in a decrease in the amount of EphA2 associated with total Src (Fig. 6, D). To determine whether the decreased Src activity after EA5 treatment was due to a decrease in phosphorylated Src specifically associated with EphA2, phosphorylated Src^{Y419} ($pSrc^{Y419}$) was immunoprecipitated using anti–total Src and

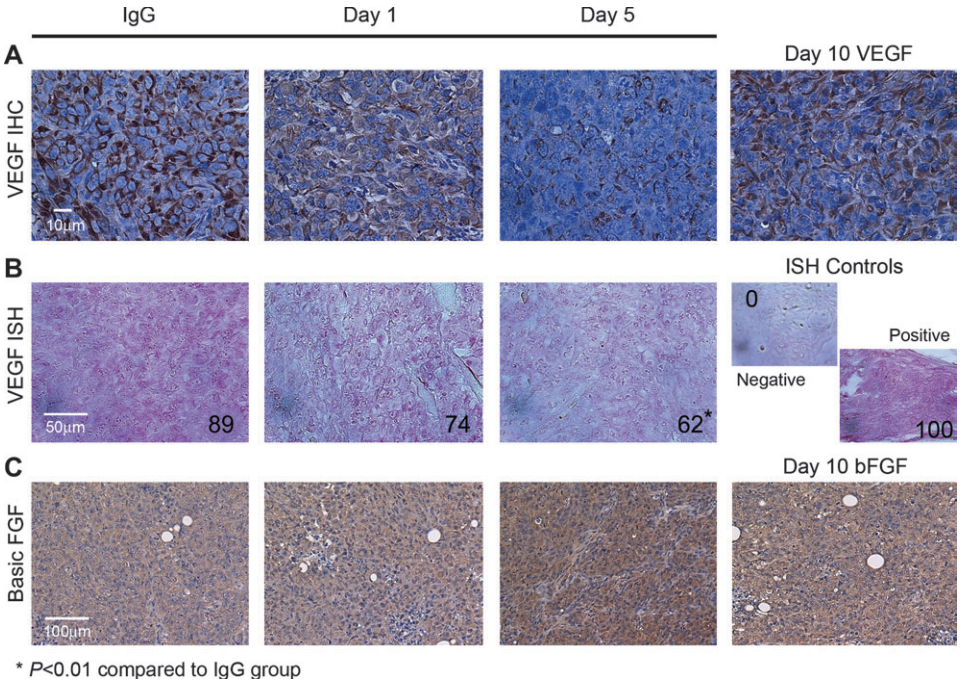

Fig. 5. Immunohistochemical analysis of vascular endothelial growth factor (VEGF) and basic fibroblast growth factor (bFGF) expression in EA5-treated mice. Mice (n = 8) bearing intraperitoneal HeyA8 tumors, 17 days after intraperitoneal cell injection, were treated with two doses of 10 mg/kg EA5 or IgG (at days 0 and 3). Mice were killed 24 hours after the first dose (day 1), 48 hours after the second dose (day 5), or 7 days after the second dose (day 10) and tumors harvested. **A**) Immunohistochemical analysis of tumor samples for VEGF protein by immunohistochemistry. **B**) In situ hybridization analysis of tumor samples for VEGF RNA. **C**) Immunohistochemical analysis of tumor samples for bFGF protein. Numbers in (**B**) indicate mean relative values of staining intensity, on a scale in which the negative control was assigned a value of zero and positive control a value of 100, from four photographs, with 10 random fields on each slide selected for intensity analysis. The 95% confidence intervals for all groups ranged from 1.2 to 3.1, comparisons made with student's *t* test and analysis of variance.

precipitates were immunoblotted for EphA2. In SKOV3ip1 cells that were treated with control IgG, EphA2 coimmunoprecipitated with Src^{Y419} (Fig. 6, E). However, in cells that were treated with EA5, no coimmunoprecipitation of $pSrc^{Y419}$ with EphA2 was observed. This observation suggests that EA5 treatment led to a reduction in phosphorylated Src activity in EphA2 complexes. Finally, the expression of a candidate Src-targeting phosphatase, PTP-BAS, which may contribute to Src dephosphorylation, was examined in SKOV3ip1 cells. Untreated cells were subjected to immunoprecipitation with anti–PTP-BAS, followed by immunoblotting for EphA2 and PTP-BAS expression. EphA2 was found to be associated with PTP-BAS (Fig. 6, F). Collectively, these data indicate that EA5-induced reduction in EphA2 levels reduced Src phosphorylation and contributed to a secondary decrease in VEGF expression.

Discussion

In this study, we found that use of an agonistic antibody that leads to a reduction in EphA2 levels, in combination with paclitaxel, substantially reduced tumor growth in an ovarian cancer model, including a paclitaxel-resistant model. These effects appeared to be due, at least in part, to a decrease in VEGF expression, decreased proliferation, and decreased microvessel density through induction of apoptosis in tumor-associated endothelial cells. The decreased VEGF expression appeared to result, at least in part, from decreased levels of phosphorylated Src after dissociation from EphA2.

One novel finding of our study is that an EphA2-agonistic antibody could reduce the growth of ovarian tumors. This result is consistent with recent EphA2-targeting studies, in which a decrease in EphA2 expression by treatment with an agonistic antibody led to inhibition of breast tumor growth *(33)* and siRNA-mediated reduction in EphA2 expression led to inhibition of growth in pancreatic and ovarian cancer models *(32,34)*. We further found that a reduction in EphA2 levels can increase host survival. The mechanism of antitumor effects of EphA2 were further delineated with our finding that VEGF levels were reduced in parallel with dissociation of EphA2 from the Src oncoprotein. Previous studies have shown that Src activation is critical for VEGF expression in ovarian tumor cells both in vitro and in vivo *(50)*. Thus, EphA2-agonistic antibodies may be particularly beneficial for targeting a population of tumor cells—i.e., VEGF-producing cells—that contribute to angiogenesis and progressive tumor growth.

The mechanism by which reduced expression of EphA2 is achieved does not appear to be crucial to its ability to inhibit growth in the murine ovarian cancer model. The EA5-agonistic antibody reduced EphA2 expression by induced phosphorylation of the EphA2 receptor, followed by internalization and destruction *(33)*. EA5-induced EphA2 phosphorylation also activates other pathways, such as the mitogen-activated protein kinase pathway *(51)*. By contrast, siRNA therapy prevents translation of EphA2 without activation of the receptor and subsequent receptor-induced pathways. Nevertheless, siRNA therapy led to a similar reduction in growth in the murine preclinical model, both alone and in combination with paclitaxel *(32)*. Therefore, one of the most important aspects of anti-EphA2 therapy may be a reduction in the absolute levels of membrane-bound EphA2.

Antibody-mediated reduction of EphA2 levels is attractive for prolonged therapy, where a favorable balance between efficacy and toxicity is essential for several reasons. First, EphA2 is expressed in only a few normal epithelial tissues, at low levels *(11)*, which should translate to decreased toxicity and a greater therapeutic window. Second, the selectivity of antibody-based therapies may make antibodies superior to other therapies, such as small molecule inhibitors, which often affect multiple targets, thereby increasing the risk of side effects. Third, the EphA2-agonistic antibody tested functions to restore a signal that is normally provided by receptor–ligand binding, which is lost in most cancer cells due to poor receptor–ligand interactions. The loss of this signal arises because EphA2 normally binds ephrin-A1, which is anchored to the membrane of adjacent cells. However, tumor cells often have unstable intercellular contacts, which

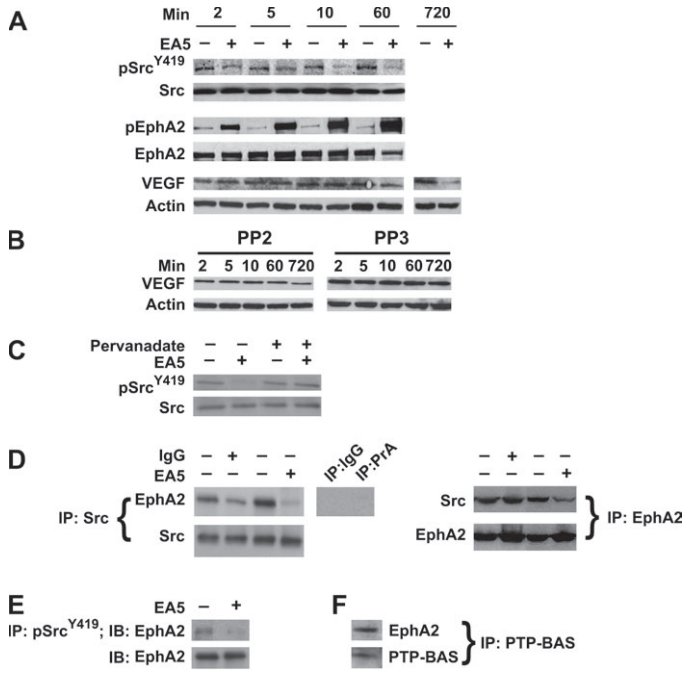

Fig. 6. Effect of EA5 treatment of SKOV3ip1 ovarian cancer cells in vitro on Src. **A**) HeyA8 cells were treated with 10 μg/mL of either nonspecific IgG or EA5 for the indicated periods of time. Immunoblotting was performed for phosphorylated Src^{Y419} ($pSrc^{Y419}$), total Src, phosphorylated EphA2 (pEphA2), EphA2, vascular endothelial growth factor (VEGF), and actin. **B**) Cells were treated with the Src inhibitor PP2 (10 μM) or its inactive form, PP3 (10 μM) for the indicated times followed by immunoblotting for VEGF and actin. **C**) Cells were pretreated for 5 minutes with pervanadate or vehicle control and then treated with EA5 for 10 minutes. Immunoblotting was performed for $pSrc^{Y419}$ and, after stripping, for total Src. **D**) Cells were treated with control IgG or EA5 for 10 minutes, and lysates were subjected to immunoprecipitation (IP) for Src (left) or EphA2 (right) followed by immunoblotting for EphA2 and Src. For controls, immunoprecipitation with isotype control antibody (IgG) and protein A sepharose beads (PrA) alone was also performed. **E**) Cells treated with either control IgG or EA5 were lysed and immunoprecipitated with an antibody to $pSrc^{Y419}$, and immunoprecipitates were analyzed by EphA2 immunoblotting. Separate immunoblots for EphA2 was performed from the same cell lysate (i.e., not immunoprecipitated). **F**) Untreated cells were immunoprecipitated with an antibody for PTP-BAS followed by immunoblotting for EphA2 and PTP-BAS. Results were confirmed with a second identically performed experiment and separate immunoprecipitation/immunoblot.

reduces the binding efficiency of EphA2 and its ligand *(9)*. The biologic consequences of this alteration are profound because ligand-bound EphA2 transmits signals that negatively regulate tumor cell growth and migration and is then internalized and degraded. In contrast, without ligand binding, EphA2 positively regulates these same behaviors in tumor cells, and the lack of internalization allows EphA2 to accumulate at the cell surface and convey continuous promalignant signals *(20)*. This knowledge formed the basis for the studies reported here, in which we sought to mimic the biologic and biochemical consequences of stable ligand binding using an agonistic monoclonal antibody. Finally, ovarian cancer is highly responsive to chemotherapy, and the high proliferation rate of ovarian cancer cells should make them susceptible to growth-modulating therapies. Consolidation therapy with chemotherapy has been shown to prolong progression-free survival *(52)*. If EphA2 reduction proves to have a favorable side effect profile, its use could hold promise in a prolonged consolidation setting.

We observed substantial reductions in tumor growth in mice treated with the EphA2-agonistic antibody in combination with paclitaxel, despite a lack of in vitro effects of the combination on cell proliferation. Other investigators have also reported that EphA2 reduction had a similar lack of effects in monolayer culture but inhibited growth in three-dimensional cultures *(33,53)*. Many factors can affect growth in vivo that are not present in monolayer culture, including the complexity of the extracellular matrix, vascularization, heterogeneity of cell types, circulating growth factors, and variations in signaling that result from growth in three-dimensional models. Given the role of EphA2 in cell migration and signaling through the extracellular matrix, it is plausible that EphA2 reduction would have important effects in vivo that are not seen in vitro. Indeed, in each of the in vivo trials reported here, EphA2 reduction in combination with paclitaxel was more effective than paclitaxel alone.

Recent studies have shown a functional relationship between VEGF and EphA2, but most of these studies have focused on the role of these molecules on endothelial cell behavior. For example, selective targeting of EphA2 prevents endothelial cells from responding fully to VEGF and thereby negatively regulates endothelial cell migration *(42,43,45)*, sprouting *(42)*, and survival *(42)*. Similarly, it has been shown that VEGF induces ephrin-A1 production and that many of VEGF's effects proceed through the EphA2 receptor *(42)*. To the best of our knowledge, our finding that reduced EphA2 in tumor cells leads to decreased VEGF expression provides the first evidence that EphA2 is not just a mediator of VEGF effects but also influences VEGF expression. The reduction in VEGF with reduced EphA2 appears to be mediated, at least in part, by decreasing activity of Src, which is known to regulate VEGF expression by tumor cells *(54,55)*. Specifically, we demonstrated that EA5 treatment led to dissociation of Src from EphA2, resulting in decreased phosphorylation of Src on Tyr-419. Src dephosphorylation was blocked by phosphatase inhibitors, which indicates the requirement for a phosphatase. A candidate phosphatase, PTP-BAS (also known as FAP-1), which is known to be expressed in ovarian cancers *(56)* and to dephosphorylate $pSrc^{Y419}$ *(57)*, was found to be physically associated with EphA2 (Fig. 6, F). Our findings therefore suggest a novel mechanism for EphA2 targeting, in which activation of EphA2 by an agonistic antibody and the subsequent reduction in its levels result in Src dephosphorylation and decreased tumor angiogenesis.

The observed antivascular activity of EA5 is further supported by its induction of endothelial cell apoptosis and reduced number of tumor-associated endothelial cells. These effects are likely related to decreased levels of VEGF, which is generally understood to function as a survival factor for endothelial cells *(58,59)*. For example, inhibiting phosphorylation of the VEGF receptor sensitizes tumor-associated endothelial cells to cytotoxic agents, leading to apoptosis *(60)*. However, direct endothelial cell regression has also been shown by more direct VEGF targeting, such as using VEGF-Trap to bind VEGF and prevent its activity *(61)*. Here, the reduction in EphA2 acted indirectly on endothelial cells by leading to depletion of tumor-produced VEGF. In addition, agonistic EphA2 antibodies can directly trigger the death of tumor cells, as was demonstrated previously in both pancreatic tumor cells *(43,45)* and endothelial cells *(43)*. Notably, these particular experiments were conducted with EphA2 targeting alone, not with combination chemotherapy, and so it was not the case that EphA2 inhibition was simply allowing taxanes to induce apoptosis. It is tempting to speculate that EphA2 reduction may also affect vasculogenic mimicry, whereby aggressive tumor cells

take on the properties of endothelial cells and can line tubular structures that carry blood into tumors. This phenomenon has been demonstrated in ovarian and other cancers *(62,63)*, and EphA2 plays a functional role in the ability of aggressive tumor cells to form extracellular matrix-rich vasculogenic-like networks in three-dimensional culture *(64,65)*. It is possible that EphA2 targeting decreases microvessel density by affecting both tumor-associated endothelial cells and those tumor cells that adopt an endothelial-like phenotype.

Limitations of this study include those inherent to preclinical studies, including using a finite number of cell lines that may have less variability than the myriad of patients with ovarian cancer and use of athymic mice that have a different immune response than human patients. Additionally, the therapeutic antibody used in this study recognizes only human EphA2. Although recognition of EphA2 on both tumor cells and endothelial cells may allow even greater therapeutic efficacy, it may also lead to toxicities not seen in the mouse model.

In summary, the findings herein provide a new understanding of EphA2 function in tumor cells and suggest that selective targeting of molecules on tumor cells can have direct effects on the tumor while concomitantly depriving the microvasculature of an essential survival factor. Combining EphA2-agonistic antibodies with cytotoxic agents further enhanced this dual mechanism. Future investigation will be necessary to determine whether this strategy will translate into a new opportunity for clinical intervention against the large number of tumors that overexpress EphA2, most notably ovarian cancer.

References

(1) Jemal A, Siegel R, Ward E, Murray T, Xu J, Smigal C, et al. Cancer statistics, 2006. CA Cancer J Clin 2006;56:106–30.

(2) Lister-Sharp D, McDonagh MS, Khan KS, Kleijnen J. A rapid and systematic review of the effectiveness and cost-effectiveness of the taxanes used in the treatment of advanced breast and ovarian cancer. Health Technol Assess 2000;4(17):1–113.

(3) Hoskins W, Perez C, Young R, Barakat R, Markman M, Randall M. Principles and practice of gynecologic oncology. 4th ed. Philadelphia (PA): Lippincott Williams & Wilkins; 2005.

(4) Hurwitz H, Fehrenbacher L, Novotny W, Cartwright T, Hainsworth J, Heim W, et al. Bevacizumab plus irinotecan, fluorouracil, and leucovorin for metastatic colorectal cancer. N Engl J Med 2004;350:2335–42.

(5) Ferrara N, Hillan KJ, Gerber HP, Novotny W. Discovery and development of bevacizumab, an anti-VEGF antibody for treating cancer. Nat Rev Drug Discov 2004;3:391–400.

(6) Tripathy D, Slamon DJ, Cobleigh M, Arnold A, Saleh M, Mortimer JE, et al. Safety of treatment of metastatic breast cancer with trastuzumab beyond disease progression. J Clin Oncol 2004;22:1063–70.

(7) Caponigro F, Formato R, Caraglia M, Normanno N, Iaffaioli RV. Monoclonal antibodies targeting epidermal growth factor receptor and vascular endothelial growth factor with a focus on head and neck tumors. Curr Opin Oncol 2005;17:212–7.

(8) Nakamoto M, Bergemann AD. Diverse roles for the Eph family of receptor tyrosine kinases in carcinogenesis. Microsc Res Tech 2002;59:58–67.

(9) Kinch MS, Carles-Kinch K. Overexpression and functional alterations of the EphA2 tyrosine kinase in cancer. Clin Exp Metastasis 2003;20:59–68.

(10) Ireton RC, Chen J. EphA2 receptor tyrosine kinase as a promising target for cancer therapeutics. Curr Cancer Drug Targets 2005;5:149–57.

(11) Lindberg RA, Hunter T. cDNA cloning and characterization of eck, an epithelial cell receptor protein-tyrosine kinase in the eph/elk family of protein kinases. Mol Cell Biol 1990;10:6316–24.

(12) Gale NW, Holland SJ, Valenzuela DM, Flenniken A, Pan L, Ryan TE, et al. Eph receptors and ligands comprise two major specificity subclasses and are reciprocally compartmentalized during embryogenesis. Neuron 1996;17:9–19.

(13) Flanagan JG, Vanderhaeghen P. The ephrins and Eph receptors in neural development. Annu Rev Neurosci 1998;21:309–45.

(14) Chen J, Nachabah A, Scherer C, Ganju P, Reith A, Bronson R, et al. Germline inactivation of the murine Eck receptor tyrosine kinase by gene trap retroviral insertion. Oncogene 1996;12:979–88.

(15) Andres AC, Reid HH, Zurcher G, Blaschke RJ, Albrecht D, Ziemiecki A. Expression of two novel eph-related receptor protein tyrosine kinases in mammary gland development and carcinogenesis. Oncogene 1994;9:1461–7.

(16) Ganju P, Shigemoto K, Brennan J, Entwistle A, Reith AD. The Eck receptor tyrosine kinase is implicated in pattern formation during gastrulation, hindbrain segmentation and limb development. Oncogene 1994;9:1613–24.

(17) Pandey A, Duan H, Dixit VM. Characterization of a novel Src-like adapter protein that associates with the Eck receptor tyrosine kinase. J Biol Chem 1995;270:19201–4.

(18) Pandey A, Shao H, Marks RM, Polverini PJ, Dixit VM. Role of B61, the ligand for the Eck receptor tyrosine kinase, in TNF-alpha-induced angiogenesis. Science 1995;268:567–9.

(19) Rosenberg IM, Goke M, Kanai M, Reinecker HC, Podolsky DK. Epithelial cell kinase-B61: an autocrine loop modulating intestinal epithelial migration and barrier function. Am J Physiol 1997;273(Pt 1):G824–32.

(20) Zelinski DP, Zantek ND, Stewart JC, Irizarry AR, Kinch MS. EphA2 overexpression causes tumorigenesis of mammary epithelial cells. Cancer Res 2001;61:2301–6.

(21) Lu M, Miller KD, Gokmen-Polar Y, Jeng MH, Kinch MS. EphA2 overexpression decreases estrogen dependence and tamoxifen sensitivity. Cancer Res 2003;63:3425–9.

(22) D'Amico TA, Aloia TA, Moore MB, Conlon DH, Herndon JE 2nd, Kinch MS, et al. Predicting the sites of metastases from lung cancer using molecular biologic markers. Ann Thorac Surg 2001;72:1144–8.

(23) Ogawa K, Pasqualini R, Lindberg RA, Kain R, Freeman AL, Pasquale EB. The ephrin-A1 ligand and its receptor, EphA2, are expressed during tumor neovascularization. Oncogene 2000;19:6043–52.

(24) Fox BP, Kandpal RP. Invasiveness of breast carcinoma cells and transcript profile: Eph receptors and ephrin ligands as molecular markers of potential diagnostic and prognostic application. Biochem Biophys Res Commun 2004;318:882–92.

(25) Walker-Daniels J, Coffman K, Azimi M, Rhim JS, Bostwick DG, Snyder P, et al. Overexpression of the EphA2 tyrosine kinase in prostate cancer. Prostate 1999;41:275–80.

(26) Kataoka H, Igarashi H, Kanamori M, Ihara M, Wang JD, Wang YJ, et al. Correlation of EPHA2 overexpression with high microvessel count in human primary colorectal cancer. Cancer Sci 2004;95:136–41.

(27) Duxbury MS, Ito H, Zinner MJ, Ashley SW, Whang EE. EphA2: a determinant of malignant cellular behavior and a potential therapeutic target in pancreatic adenocarcinoma. Oncogene 2004;23:1448–56.

(28) Easty DJ, Bennett DC. Protein tyrosine kinases in malignant melanoma. Melanoma Res 2000;10:401–11.

(29) Nemoto T, Ohashi K, Akashi T, Johnson JD, Hirokawa K. Overexpression of protein tyrosine kinases in human esophageal cancer. Pathobiology 1997;65:195–203.

(30) Thaker PH, Deavers M, Celestino J, Thornton A, Fletcher MS, Landen CN, et al. EphA2 expression is associated with aggressive features in ovarian carcinoma. Clin Cancer Res 2004;10:5145–50.

(31) Miao H, Burnett E, Kinch M, Simon E, Wang B. Activation of EphA2 kinase suppresses integrin function and causes focal-adhesion-kinase dephosphorylation. Nat Cell Biol 2000;2:62–9.

(32) Landen CN Jr, Chavez-Reyes A, Bucana C, Schmandt R, Deavers MT, Lopez-Berestein G, et al. Therapeutic EphA2 gene targeting in vivo using neutral liposomal small interfering RNA delivery. Cancer Res 2005;65:6910–8.

(33) Carles-Kinch K, Kilpatrick KE, Stewart JC, Kinch MS. Antibody targeting of the EphA2 tyrosine kinase inhibits malignant cell behavior. Cancer Res 2002;62:2840–7.

(34) Duxbury MS, Matros E, Ito H, Zinner MJ, Ashley SW, Whang EE. Systemic siRNA-mediated gene silencing: a new approach to targeted therapy of cancer. Ann Surg 2004;240:667–74; discussion 675–6.

(35) Parker MA, Brantley-Sieders DM, Fang WB, Chen J. Ephrin-A1 induces tumor cell migration via a Rho GTPase and Jak kinase-dependent pathway. Proc Am Assoc Cancer Res 2005; Abstract#5471.
(36) Apte SM, Bucana CD, Killion JJ, Gershenson DM, Fidler IJ. Expression of platelet-derived growth factor and activated receptor in clinical specimens of epithelial ovarian cancer and ovarian carcinoma cell lines. Gynecol Oncol 2004;93:78–86.
(37) Langley RR, Ramirez KM, Tsan RZ, Van Arsdall M, Nilsson MB, Fidler IJ. Tissue-specific microvascular endothelial cell lines from H-2K(b)-tsA58 mice for studies of angiogenesis and metastasis. Cancer Res 2003;63:2971–6.
(38) Baker CH, Solorzano CC, Fidler IJ. Blockade of vascular endothelial growth factor receptor and epidermal growth factor receptor signaling for therapy of metastatic human pancreatic cancer. Cancer Res 2002;62:1996–2003.
(39) Solorzano CC, Baker CH, Tsan R, Traxler P, Cohen P, Buchdunger E, et al. Optimization for the blockade of epidermal growth factor receptor signaling for therapy of human pancreatic carcinoma. Clin Cancer Res 2001;7: 2563–72.
(40) Abraham S, Knapp DW, Cheng L, Snyder PW, Mittal SK, Bangari DS, et al. Expression of EphA2 and Ephrin A-1 in carcinoma of the urinary bladder. Clin Cancer Res 2006;12:353–60.
(41) Bookman MA, McGuire WP 3rd, Kilpatrick D, Keenan E, Hogan WM, Johnson SW, et al. Carboplatin and paclitaxel in ovarian carcinoma: a phase I study of the Gynecologic Oncology Group. J Clin Oncol 1996;14:1895–902.
(42) Cheng N, Brantley DM, Liu H, Lin Q, Enriquez M, Gale N, et al. Blockade of EphA receptor tyrosine kinase activation inhibits vascular endothelial cell growth factor-induced angiogenesis. Mol Cancer Res 2002;1:2–11.
(43) Cheng N, Brantley D, Fang WB, Liu H, Fanslow W, Cerretti DP, et al. Inhibition of VEGF-dependent multistage carcinogenesis by soluble EphA receptors. Neoplasia 2003;5:445–56.
(44) Dobrzanski P, Hunter K, Jones-Bolin S, Chang H, Robinson C, Pritchard S, et al. Antiangiogenic and antitumor efficacy of EphA2 receptor antagonist. Cancer Res 2004;64:910–9.
(45) Brantley DM, Cheng N, Thompson EJ, Lin Q, Brekken RA, Thorpe PE, et al. Soluble Eph A receptors inhibit tumor angiogenesis and progression in vivo. Oncogene 2002;21:7011–26.
(46) Saito T, Masuda N, Miyazaki T, Kanoh K, Suzuki H, Shimura T, et al. Expression of EphA2 and E-cadherin in colorectal cancer: correlation with cancer metastasis. Oncol Rep 2004;11:605–11.
(47) Ellis LM, Staley CA, Liu W, Fleming RY, Parikh NU, Bucana CD, et al. Down-regulation of vascular endothelial growth factor in a human colon carcinoma cell line transfected with an antisense expression vector specific for c-src. J Biol Chem 1998;273:1052–7.
(48) Summy JM, Trevino JG, Baker CH, Gallick GE. c-Src regulates constitutive and EGF-mediated VEGF expression in pancreatic tumor cells through activation of phosphatidyl inositol-3 kinase and p38 MAPK. Pancreas 2005;31:263–74.
(49) Han L, Landen C, Trevino J, Halden J, Lin Y, Kamat A, et al. Anti-angiogenic and anti-tumor effects of Src inhibition in ovarian carcinoma. Cancer Res 2006;66:8633–9.
(50) Wiener JR, Nakano K, Kruzelock RP, Bucana CD, Bast RC Jr, Gallick GE. Decreased Src tyrosine kinase activity inhibits malignant human ovarian cancer tumor growth in a nude mouse model. Clin Cancer Res 1999;5: 2164–70.
(51) Pratt RL, Kinch MS. Activation of the EphA2 tyrosine kinase stimulates the MAP/ERK kinase signaling cascade. Oncogene 2002;21:7690–9.
(52) Markman M, Liu PY, Wilczynski S, Monk B, Copeland LJ, Alvarez RD, et al. Phase III randomized trial of 12 versus 3 months of maintenance paclitaxel in patients with advanced ovarian cancer after complete response to platinum and paclitaxel-based chemotherapy: a Southwest Oncology Group and Gynecologic Oncology Group trial. J Clin Oncol 2003;21: 2460–5.
(53) Potla L, Boghaert ER, Armellino D, Frost P, Damle NK. Reduced expression of EphrinA1 (EFNA1) inhibits three-dimensional growth of HT29 colon carcinoma cells. Cancer Lett 2002;175:187–95.
(54) Gray MJ, Zhang J, Ellis LM, Semenza GL, Evans DB, Watowich SS, et al. HIF-1alpha, STAT3, CBP/p300 and Ref-1/APE are components of a transcriptional complex that regulates Src-dependent hypoxia-induced expression of VEGF in pancreatic and prostate carcinomas. Oncogene 2005;24:3110–20.
(55) Summy JM, Gallick GE. Treatment for advanced tumors: SRC reclaims center stage. Clin Cancer Res 2006;12:1398–401.
(56) Meinhold-Heerlein I, Stenner-Liewen F, Liewen H, Kitada S, Krajewska M, Krajewski S, et al. Expression and potential role of Fas-associated phosphatase-1 in ovarian cancer. Am J Pathol 2001;158:1335–44.
(57) Roskoski R Jr. Src kinase regulation by phosphorylation and dephosphorylation. Biochem Biophys Res Commun 2005;331:1–14.
(58) Watanabe Y, Dvorak HF. Vascular permeability factor/vascular endothelial growth factor inhibits anchorage-disruption-induced apoptosis in microvessel endothelial cells by inducing scaffold formation. Exp Cell Res 1997;233:340–9.
(59) Dvorak HF. Vascular permeability factor/vascular endothelial growth factor: a critical cytokine in tumor angiogenesis and a potential target for diagnosis and therapy. J Clin Oncol 2002;20:4368–80.
(60) Thaker PH, Yazici S, Nilsson MB, Yokoi K, Tsan RZ, He J, et al. Antivascular therapy for orthotopic human ovarian carcinoma through blockade of the vascular endothelial growth factor and epidermal growth factor receptors. Clin Cancer Res 2005;11:4923–33.
(61) Ouchi M, Fujiuchi N, Sasai K, Katayama H, Minamishima YA, Ongusaha PP, et al. BRCA1 phosphorylation by Aurora-A in the regulation of G2 to M transition. J Biol Chem 2004;279:19643–8.
(62) Sood AK, Seftor EA, Fletcher MS, Gardner LM, Heidger PM, Buller RE, et al. Molecular determinants of ovarian cancer plasticity. Am J Pathol 2001;158:1279–88.
(63) Sood AK, Fletcher MS, Coffin JE, Yang M, Seftor EA, Gruman LM, et al. Functional role of matrix metalloproteinases in ovarian tumor cell plasticity. Am J Obstet Gynecol 2004;190:899–909.
(64) Hendrix MJ, Seftor EA, Hess AR, Seftor RE. Molecular plasticity of human melanoma cells. Oncogene 2003;22:3070–5.
(65) Hendrix MJ, Seftor EA, Kirschmann DA, Quaranta V, Seftor RE. Remodeling of the microenvironment by aggressive melanoma tumor cells. Ann N Y Acad Sci 2003;995:151–61.

Notes

This research was funded in part by the Bettyann Asche-Murray Fellowship Award at the University of Texas M. D. Anderson Cancer Center to C. N. Landen; the Gillson Longenbaugh Foundation Award to G. E. Gallick; and grants from the Department of Defense #W81XWH-04-1-0227, the Marcus Foundation, and the University of Texas M. D. Anderson Cancer Center SPORE in ovarian cancer #2P50CA083639 awarded to A. K. Sood. The study sponsors had no role in the design of the study, the collection and analyses of data, the writing of the study, or the decision to publish.

The authors would like to thank Drs Isaiah J. Fidler, Dominic Fan, and Honnavara Ananthaswamy for their helpful input and discussions regarding this work. The authors also thank Dr Edward N. Atkinson (Department of Biostatistics and Applied Mathematics, M. D. Anderson Cancer Center) for help with statistical analyses. The authors also thank Corazon Bucana and Donna Reynolds for assistance with immunohistochemistry.

Manuscript received February 16, 2006; revised August 18, 2006; accepted September 8, 2006.